Erik Jonsson School of Engineering and Computer Science

Decoupling the Influence of Surface Structure and Intrinsic Wettability on Boiling Heat Transfer—Supplement

UT Dallas Author(s):

Xianming (Simon)Dai

Citation:

Dai, X., P. Wang, F. Yang, X. Li, et al. 2018. "Decoupling the influence of surface structure and intrinsic wettability on boiling heat transfer." Applied Physics Letters 112(25), doi:10.1063/1.5030420

Decoupling the Influence of Surface Structure and Intrinsic Wettability on Boiling Heat Transfer

Xianming Dai,[1,2,a)] Pengtao Wang,[1,a)] Fanghao Yang,[1)] Xiaochuan Li,[3)] and Chen Li[1, b)]

[1]Department of Mechanical Engineering, University of South Carolina, Columbia, South Carolina 29208, USA

[2]Department of Mechanical Engineering, University of Texas at Dallas, Richardson, Texas 75080, USA

[3]School of Hydraulic, Energy and Power Engineering, Yangzhou University, Yangzhou, Jiangsu 225127, China

Outline of Supplemental Information:

S1. Atomic Layer deposition of TiO_2

The deposition of active material TiO_2 on the conducting copper surface was carried out in a viscous-flow, hot-wall type reactor at 150 °C and 0.9 Torr , as shown in Fig. S1[1]. Ultra-high purity N_2 was used as the carrier gas during the deposition. Prior to TiO_2 deposition, Al_2O_3 was pre-deposited as a seed layer to facilitate TiO_2 nucleation and growth, which ensures the conformality of ALD TiO_2 coatings. The surface chemistry during ALD process can be described

[a] Equal contributors.

[b] Corresponding author: li01@cec.sc.edu

as a binary reaction in sequence. Trimethylaluminum (TMA, $Al(CH)_3$) and water were used for ALD Al_2O_3 coating[2]

$$\mathbf{Al-OH^{*}+Al(CH_3)_3 \rightarrow Al-O-Al(CH_3)_2^{*}+CH_4} \quad \text{(S-1)}$$

$$\mathbf{Al-CH_3^{*}+H_2O \rightarrow Al-OH^{*}+CH_4} \quad \text{(S-2)}$$

Titanium tetrachloride ($TiCl_4$) and water were used for ALD TiO_2[3]

$$\mathbf{TiOH^{*}+TiCl_4 \rightarrow TiOCl_3^{*}+HCl} \quad \text{(S-3)}$$

$$\mathbf{TiCl^{*}+H_2O \rightarrow TiOH^{*}+HCl} \quad \text{(S-4)}$$

Al_2O_3 film was deposited for 50 cycles at a typical growth rate of 0.12 nm/cycle, and TiO_2 film was deposited for 320 cycles at a typical growth rate of 0.05 nm/cycle. The total film thickness of Al_2O_3/TiO_2 coating was approximately 22 nm[4].

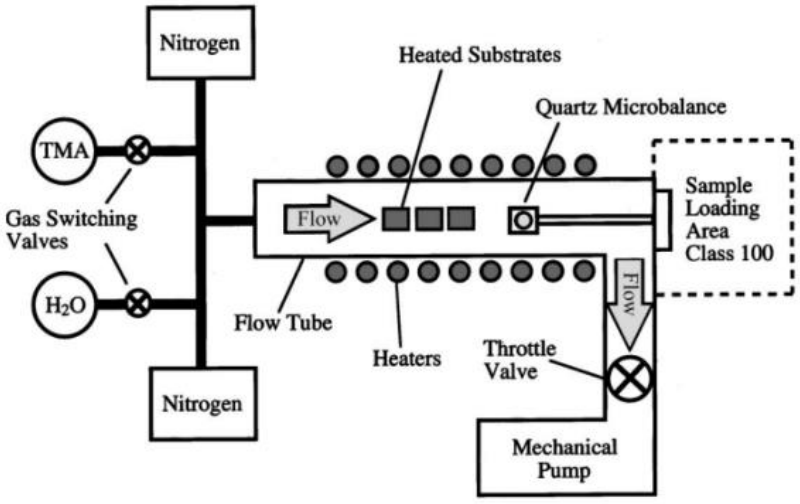

Figure S1. Schematic view of viscous flow reactor for ALD TiO_2[1].

ALD is the known best coating methods for a conformal film on high aspect ratio micro/nanostructures[5]. The ALD TiO_2 coating used in this research is prepared in Prof. Steven George's Group at the University of Colorado Boulder. The cross section of microscale copper mesh is hard to be cut with FIB, so nanowires were used to coat in the same working conditions.

After that, get the cross section of nanowire with TiO_2 coating was cut and visualized with FIB-SEM, as shown in Fig. S2. In addition, extensive information about this ALD TiO_2 coating has been reported in Ref [4, 6].

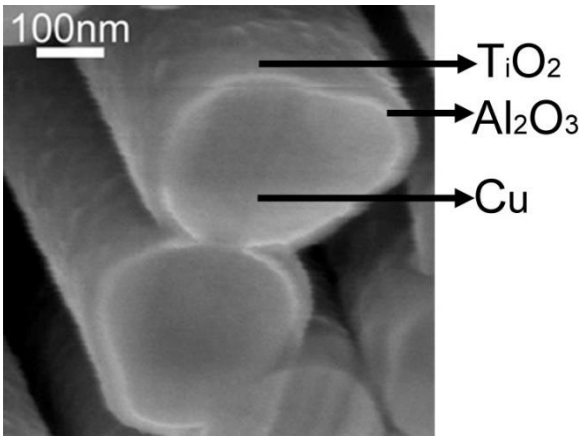

Figure S2. Cross-section SEM image of straight Ni/TiO_2 nanowire array. (Thickness of ALD TiO_2 ≈ 16 nm) (Figure 3(c) in Ref. [4])

S2. Experimental Setup

A closed system was established for experimental study (Fig. S3). An aluminum chamber was made as a reservoir. The inner walls of the chamber were coated with high temperature polyester to reduce contamination, two side walls were covered by quartz glass as observation windows, and the bottom wall was used for sample assembly. Four cartridge heaters were installed in the corners of the aluminum chamber to maintain the water temperature between 99.9 - 100.2 ºC for saturated work conditions. The temperature was accurately controlled by a proportional-integral-derivative (PID) temperature controller. A compact water heat exchanger was used to condense and recycle the vapor to keep a constant water level. A pressure gauge was installed to monitor the vapor pressure in the chamber. Additionally, the water and vapor temperature inside the chamber were measured by two T-type thermocouples. High purity water was degassed for at least 2 hours at approximately 99.9 ºC to remove non-condensable gases prior to tests.

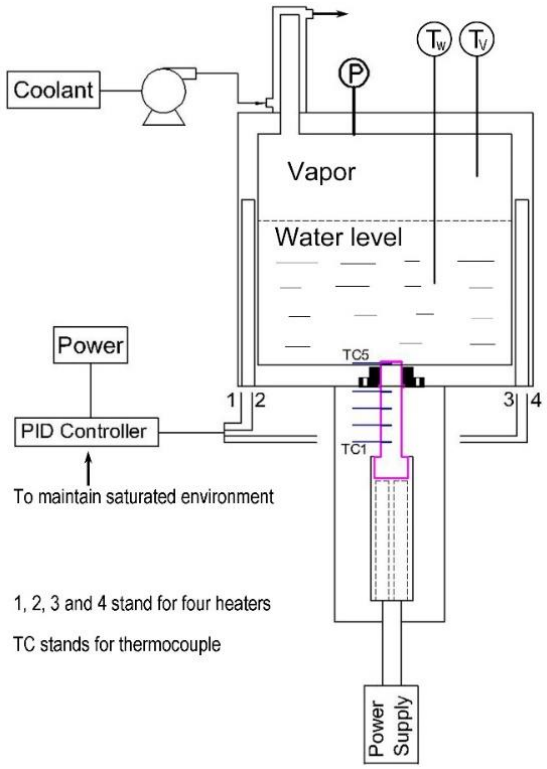

Figure S3. Experimental setup of pool boiling. TC for thermocouple; 1, 2, 3, and 4 are for heaters.

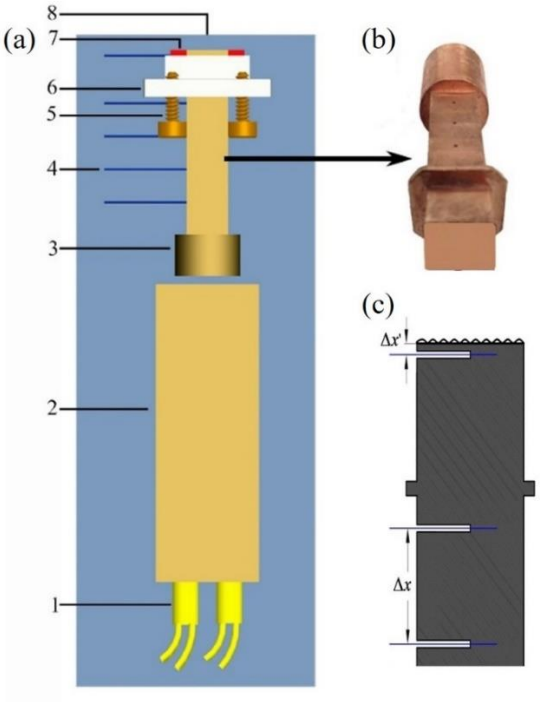

Figure S4. Schematic of the test sample. (a) Assembly of test sample. 1. Cartridge heater, 2.

Heating block, 3. TC block with holes for thermal couples, 4. K-type thermocouples, 5. Adjusting screw, 6. G-7 fiber glass, 7. High temperature RTV silicon, 8. Surface for boiling. (b) The TC block, (c) Thermalcouple arrangement and parameter for data reduction.

Copper woven meshes were sintered on a TC block with a cross-section area of 1 cm^2, where a one-dimensional (1-D) heat flux was generated. To reach a high heat flux, a pure copper heating block was made with 4 holes for heaters on one side and an opening on the other side for mount the TC block (Fig. S4(b)). Thermal grease was used to enhance the contact conditions between the heating block and the TC block. The whole heating elements were finally insulated in an aluminum housing by ceramic fiber. G-7 Fiberglass was used to insulate the TC bock to ensure the 1-D heat conduction. Power supply was used to control the input power and five K-type thermocouples (diameter 0.61mm) with linear distribution were used to estimate the input heat flux (Fig. S4 (c)). High temperature RTV silicone was used to seal the gaps between fiberglass and copper block. High temperature silicone was also used to insulate the TC block inside the chamber, the thermocouple inside the chamber and the edge of the copper woven meshes, leaving only the woven mesh surfaces in the chamber for boiling.

S3. Data reduction

Data reduction was conducted with the parameters shown in Fig. S3 (c).

$$q'' = k\frac{\Delta T}{\Delta x} \tag{S-5}$$

$$T_s = T_5 - q''\frac{\Delta x'}{k} \tag{S-6}$$

$$h = \frac{q"}{T_w - T_{sat}} \tag{S-7}$$

The uncertainties within the temperature measurements, the length or width are ± 0.5 K, ± 0.01 mm, respectively. A Monte Carlo error of propagation simulation indicated the following 95% confidence level for the computed results in most of the ranges: the heat flux was less than ± 3.2

W/cm^2; the heat transfer coefficient was less than ± 1.2 $W/(cm^2 \cdot K)$; the superheat $\Delta T = T_w - T_{sat}$ was less than ± 0.8 °C.

S4. Effects of surface structure and intrinsic wettability on boiling performance

The boiling on 2-layer-mesh and 4-layer-mesh without/with ALD TiO_2 coating are experimentally evaluated and presented as heat flux vs. superheat, HTC vs. superheat, and HTC vs. heat flux. The effects of surface structures and intrinsic wettability are shown in Figure S5 and Figure S6, respectively.

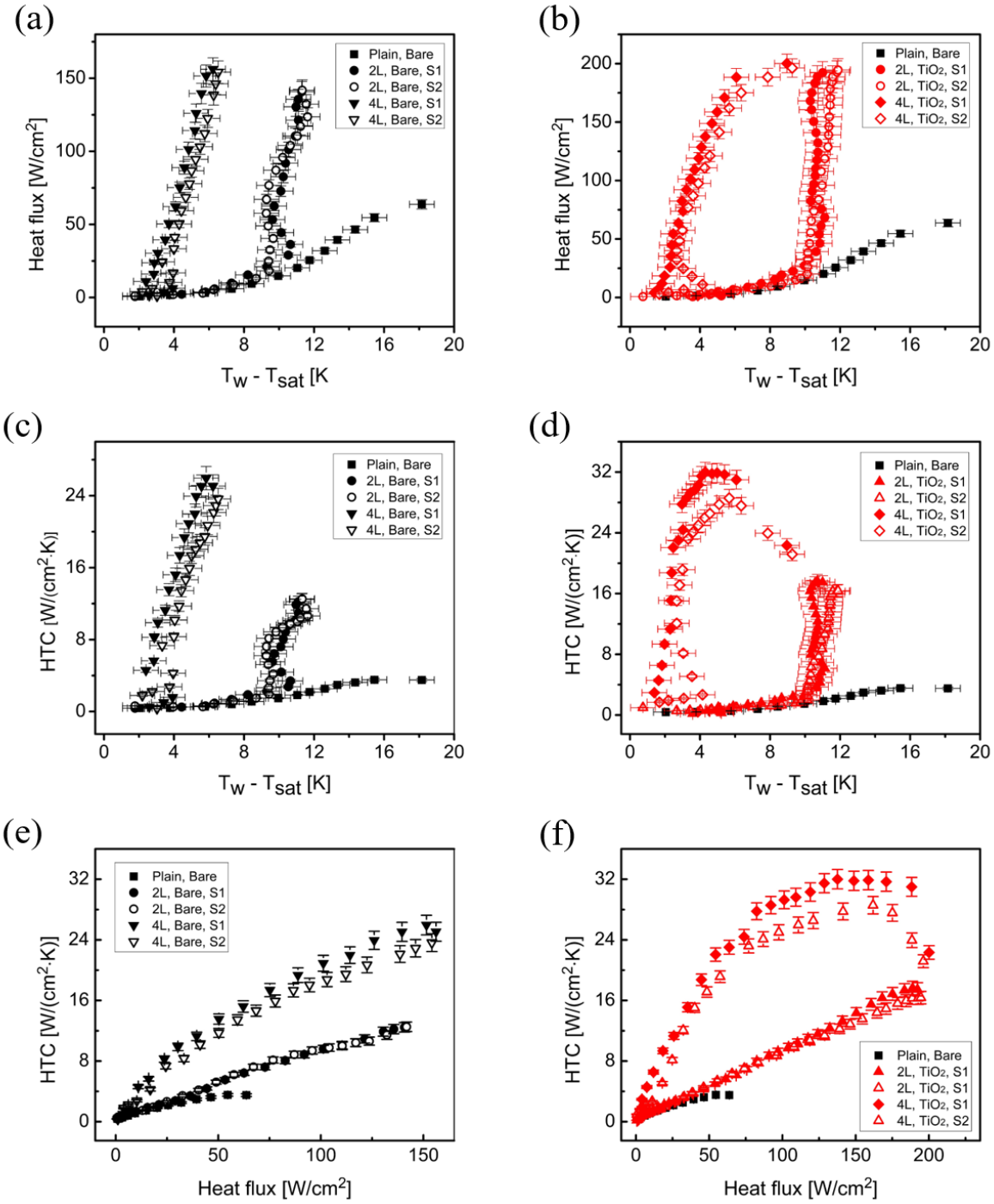

Figure S5. The effects of surface structures on the boiling heat transfer performance. Heat flux vs. wall superheat on (a) bare surface, (b) ALD TiO_2 coated surface; HTC vs. wall superheat on (c) bare surface, (d) ALD TiO_2 coated surface; HTC vs. heat flux on (e) bare surface, (f) ALD TiO_2 coated surface.

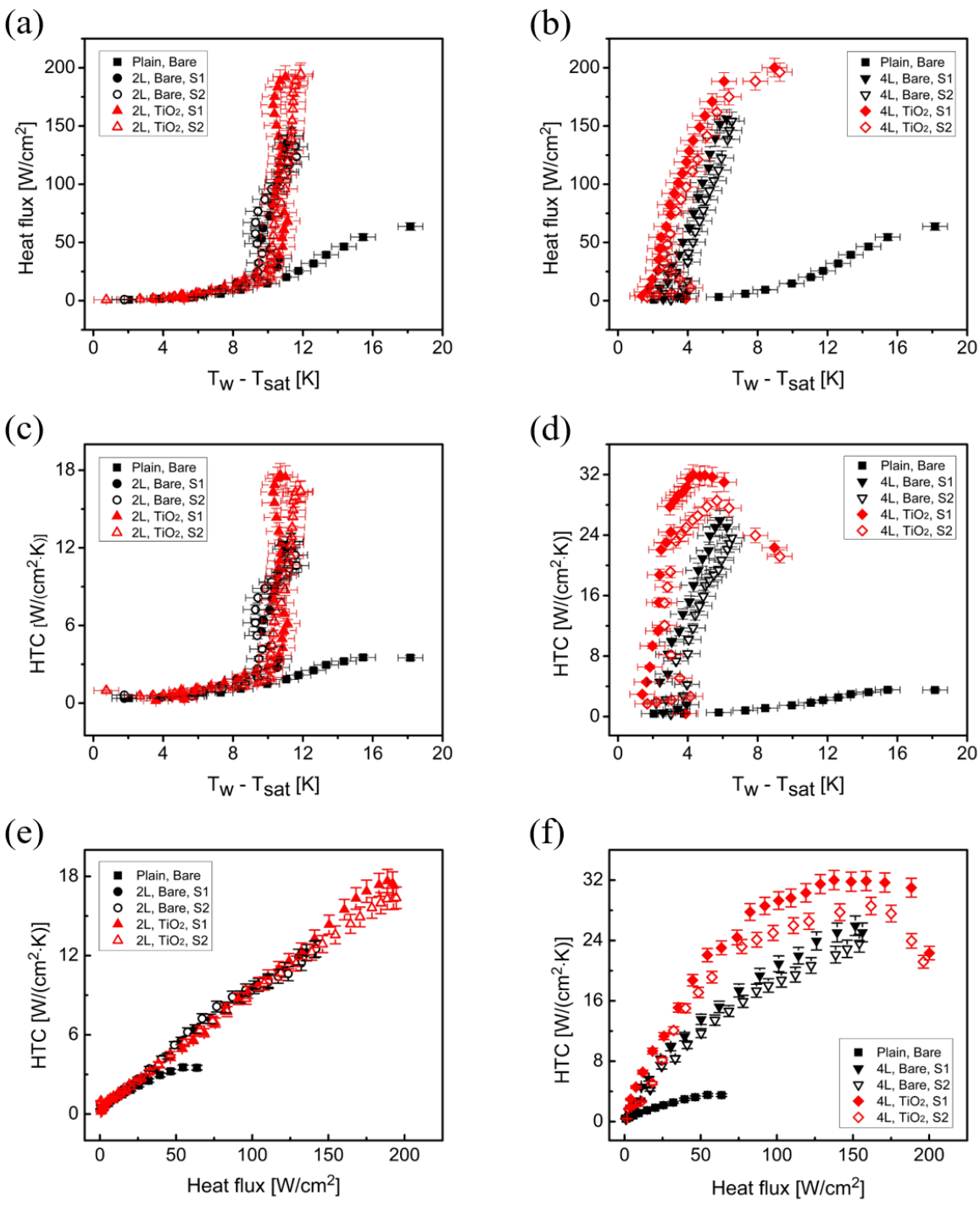

Figure S6. The effects of intrinsic wettability on the boiling heat transfer performance. Heat flux vs. wall superheat on (a) 2-layer-mesh, (b) 4-layer-mesh; HTC vs. wall superheat on (c) 2-layer-mesh, (d) 4-layer-mesh; HTC vs. heat flux on (e) 2-layer-mesh, (f) 4-layer-mesh.

S5. Analysis with empirical models for CHF

For a flat surface, ψ_{eff} = 1 and $\phi_s = 0$, Cheng's model is reduced to Kandlikar's model, where only the effect of intrinsic wettability is considered[7].

$$K_{Kandlikar} = \left(\frac{1+cos\theta}{16}\right)\left[\frac{2}{\pi} + \frac{\pi}{4}(1+\cos\theta)\right]^{1/2} \quad \text{(S-8)}$$

Kandlikar's model over predicts CHF on a plain surface, as shown in Fig 4(c), but a good agreement is achieved with Chang's model. The predicted CHF by Chang's model is 61.8 W/cm^2, while the experimental CHF is 63.7 ± 3.18 W/cm^2. Chang's model is given as[8]

$$K_{Chang} = 0.0735 \quad \text{(S-9)}$$

It is worth to note that Chang's model is based on the capillary-driven viscous flow, which may be adopted in partially considering the effects of surface structures on CHF. Kim[9] developed a CHF model based on Kandlikar's model, which introduced an additional term for the contribution of liquid spreading within nano/microstructures. Similarly, by considering the effects of intrinsic wettability on CHF with Kandlikar's model and the effects of surface structures with Chang's model, a half empirical model based on mathematical fitting of experimental data is proposed here, as

$$K_{Fitting} = K_{Kandlikar} + SK_{Chang} \quad \text{(S-10)}$$

where *S* is a constant that represents the decoupling coefficient of surface structure and intrinsic wettability, and *S* = 0.6 is proposed in this research.

Reference

[1] J.W. Elam, M.D. Groner, S.M. George, Viscous flow reactor with quartz crystal microbalance for thin film growth by atomic layer deposition, Review of Scientific Instruments, 73(8) (2002) 2981-2987.
[2] R.L. Puurunen, Surface chemistry of atomic layer deposition: A case study for the trimethylaluminum/water process, Journal of Applied Physics, 97(12) (2005) 121301.

[3] M. Ritala, M. Leskela, E. Rauhala, Atomic layer epitaxy growth of titanium dioxide thin films from titanium ethoxide, Chemistry of Materials, 6(4) (1994) 556-561.
[4] W. Wang, M. Tian, A. Abdulagatov, S.M. George, Y.-C. Lee, R. Yang, Three-Dimensional Ni/TiO2 Nanowire Network for High Areal Capacity Lithium Ion Microbattery Applications, Nano Letters, 12(2) (2012) 655-660.
[5] H. Kim, H.-B.-R. Lee, W.J. Maeng, Applications of atomic layer deposition to nanofabrication and emerging nanodevices, Thin Solid Films, 517(8) (2009) 2563-2580.
[6] A.I. Abdulagatov, Y. Yan, J.R. Cooper, Y. Zhang, Z.M. Gibbs, A.S. Cavanagh, R.G. Yang, Y.C. Lee, S.M. George, Al2O3 and TiO2 Atomic Layer Deposition on Copper for Water Corrosion Resistance, ACS Applied Materials & Interfaces, 3(12) (2011) 4593-4601.
[7] S.G. Kandlikar, A theoretical model to predict pool boiling CHF incorporating effects of contact angle and orientation, J Heat Transfer, 123 (2001).
[8] Y.P. Chang, An Analysis of the Critical Conditions and Burnout in Boiling Heat Transfer, USAEC Rep. TID-14004, Washington, DC, (1961).
[9] H.S. Ahn, H.J. Jo, S.H. Kang, M.H. Kim, Effect of liquid spreading due to nano/microstructures on the critical heat flux during pool boiling, Appl Phys Lett, 98 (2011).